https://ntrs.nasa.gov/search.jsp?R=19700025852 2018-07-24T17:16:18+00:00Z

N 70 35168

CR 109971

A MODEL FOR THE RADIATIONS FROM THE COMPACT STRONG SOURCES

CSR-TR-70-5

CENTER FOR SPACE RESEARCH
MASSACHUSETTS INSTITUTE OF TECHNOLOGY

CASE FILE COPY

A MODEL FOR THE RADIATIONS FROM THE COMPACT STRONG SOURCES

CSR-TR-70-5

A MODEL FOR THE RADIATIONS FROM THE COMPACT STRONG SOURCES

A. CAVALIERE*

Center for Space Research, Massachusetts Institute of Technology, and Laboratorio Gas Ionizzati, Frascati, Rome

P. MORRISON**

Department of Physics and Center for Space Research, Massachusetts Institute of Technology

and

F. PACINI***

Cornell-Sydney University Astronomy Center, Ithaca, New York

ABSTRACT

We present a rough but consistent model for the origins and time variations of the radiation spectrum of a typical source over all wave bands. The type example is the quasar 3C273B; we mean to include by extension various other active galactic nuclei. Primary synchrotron emission is in the infra-red; the steep decline on the low-frequency side of the power peak is due, not to self-absorption, but to the cyclotron turnover. Optical and x-ray continua are Compton-recoil photons; the radio outbursts arise in the familiar expanding clouds. The dynamical model which naturally fits the requirements is that of a condensed, rotating, magnetized body, evolving non-thermally, the spinar.

* Supported in part under an ESRO-NASA Research Associateship.

** Supported in part by NASA grants ~~NsG-106 and~~ NGL 22-009-019, and also in part by NSF Grant GP-11453.

*** Supported in part by NSF Grant GP-9621, and also in part by the Office of Naval Research, contract N-00014-67-A-0077-0007.

1. Recent observations (Kleinmann and Low 1970; Aumann and Low 1970) reinforce the inferences from previous work (Johnson and Low 1965; Low and Kleinmann 1968; Pacholczyk and Weymann 1968; Becklin and Neugebauer 1969): powerful infra-red emission is a common feature of strong radiation sources as diverse as our Galactic nucleus, the Seyfert nuclei, and the quasars. They all exhibit roughly similar spectral characteristics, a peak power in the range between a few microns to a few hundred microns wavelength, and a steep decline at both the low- and high-frequency edges. The power in the IR band often dominates any other single instrumental band, and conceivably outmeasures the whole rest of the spectrum.

Our working hypothesis is that such sources are basically IR objects. The IR emission is primary; we examine its mechanism and its relationships with the other spectral bands. The theory is still in a preliminary form, and even the observations are not complete for any single object. The model although tentative accounts consistently for what is known of the whole spectrum, and gives a rough quantitative description of all emitting regions.

2. We take as a guide for our considerations 3C273, the source perhaps best known for its overall spectrum, in keeping with the present purpose. Since unfortunately the 3C273 data are less clear just in the IR, and in addition the source is complex, some discussion is in point.[1]

---

1 We assume throughout the indicated red-shift distance, about 600 Mpc within the accuracy of the Hubble constant.

Meter band and longer wavelengths (Kellermann and Pauliny-Toth 1969; von Hoerner 1966): This emission comes largely from the very extended (10^4 pc) component 3C273A; it is constant in time. The flat power-law spectrum decreasing smoothly from a poorly-known l.f. cut-off presents no problems for a weak-field synchrotron emission mechanism. The genetic connection with 3C273 B, and the long-time energy evolution will be discussed in another paper.

Radio emission below 1m wavelength (Kellermann and Pauliny-Toth 1968): A remarkably successful picture of these emissions, which explains their composite spectrum, the time-varying intensities and downward shifting l.f. cut-offs, arises from the model of expanding plasma clouds (van der Laan 1966) emitted from time to time by a centre of activity at the optical position of 3C273 B. The clouds become detectable only after they have expanded to about 1 light month in diameter, when the internal fields are around 1 gauss; they expand visibly for a few more years, until the magnetic field reaches slowly-changing intensities, well below a milligauss. Their energy content ranges up to $\approx 10^{54}$ or 10^{55} ergs, and the mean power implied perhaps to $\approx 10^{46-47}$ erg/s. The unusual Seyfert galaxy 3C120 (NGC 1275) fits the same pattern even more quantitatively (Pauliny-Toth and Kellermann 1968).

Millimeter radiation (Kellermann, Clark, Bare et al 1968): The various expanding radio outburst clouds, resolved by interferometry as spatially compact components of the complex centimeter-band spectrum, account for the emission and its time course up to a

frequency of several times 10^{11} c/s. Just shortward of this, the radiation rises steeply with frequency, but varies in time on a scale of months or weeks. This is largely the earliest sight of the outburst clouds, with a self-absorption cut-off appropriate for the densities $\approx 1\ cm^{-3}$ and fields $\simeq 1$ Gauss. Total output from 0.3 mm to 30 m: a few 10^{46} ergs/sec.

Infra-red radiation (Kleinmann and Low 1970; Aumann and Low 1970): This wide and less-known band, which we take as extending from several hundred microns down to one micron wavelength, holds the primary emission power of 3C273B. Within its high-frequency end, from 1.1 μ to about 10 μ (the range where ground based observing is possible) the integrated power output exceeds by one order of magnitude the total radiation in all other regions, reaching say a few 10^{47} ergs/sec. There is evidence for an even larger power output, strongly varying in time, at wavelengths up to 70 μ. The emission peak must come somewhere between 20 μ and a few hundred; if it comes at the shorter wavelengths, the power is the value cited, if at the longer waves, the power goes up by one order of magnitude.

Optical continuum (Oke 1966): the falloff in frequency in the near IR is much faster than the rough $1/\nu$ behavior of the optical continuum (which is perhaps less clear in 3C273B than in other quasars). Output, about 10^{46} ergs/s from 3000 to 10000Å. Time variations on scales from weeks to decades are seen.

Optical lines (Osterbrock and Parker 1966; Burbidge and Burbidge 1967): Atomic emission lines come from a gas shell, or possibly a more filamentary structure, surrounding the source at distances of the order of tens of light years. The gas must have a mass of some 10^5 or 10^6 $M_\odot$, with these models the excitation coming either from hard photons or directly from leakage particles. The line-emitting gas shows bulk motion, whether orbital or turbulent, consistent with a large central mass, some 10^9 $M_\odot$.

X-rays: A recent experiment (Bowyer, Lampton, Mack et al 1970; Friedman 1970) has detected a power of about 1046 ergs/s from 0.2 to 10 k consistent with a $1/\nu$ extrapolation from the optical. At present resolution, however, the X-rays could originate in either or in both of the components A and B.

So active a quasar as 3C273 is perhaps unusual, but we believe that the model it implies holds also with differing parameters, for a wide range of other objects. Certainly some Seyferts also appear to be predominantly IR emitters, often with a flatter, non-thermal optical continuum (Oke 1968; Visvanathan and Oke 1968).

3. Can the IR power be made by electron synchrotron emission? Recent work (O'Dell and Sartori 1970) on synchrotron emission offers a fresh way to re-examine the issue by reconsidering the role at intermediate ($\nu > 10^{11}$ Hz) frequencies of self-absorption, which turns out not to be the origin of the l.f. cut-off.

a) Single particles of energy γmc^2 spiralling at small pitch angle θ in a magnetic field B, with $\gamma\theta > 1$, emit a synchrotron spectrum compressed within the limits:

$$\frac{\nu_B}{\gamma\theta^2} < \nu < \frac{1}{2}\nu_B\,\theta\gamma^2 \equiv \nu_u \qquad \left(\nu_B \equiv \frac{1}{2\pi}\frac{eB}{mc}\right). \qquad (1)$$

The lower limit is modified both by the increased electron mass and by the blue-shift of electrons contributing along the line of sight; the upper limit corresponds to an effective radius of curvature $\rho = \frac{2\pi c}{\nu_B}\frac{\gamma}{\theta}$ in a helicoidal orbit. The radiation pattern has a width $\Delta\psi \approx \frac{1}{\gamma}\left(\frac{\nu_u}{\nu}\right)^{1/3}$, always approaching $\Delta\psi \approx \theta$ at the lower limit.

b) For an electron energy distribution $N(\gamma) \sim \gamma^{-\sigma}$ $(\gamma_1 < \gamma < \gamma_2)$ the h.f. contributions to radiation at frequency ν give the familiar power law: $F_\nu \sim B\theta \times$ (Number of electrons with $\nu_u \approx \nu$ i.e. $(\nu/B\theta)^{-\frac{\sigma}{2}}$ $\times$ (inverse width of the radiation pattern at $\nu \approx \nu_u$ i.e. $(\nu/B\theta)^{1/2}$) $= (B\theta)^{\frac{\sigma+1}{2}}\,\nu^{-\frac{\sigma-1}{2}}$. At low frequencies $\nu \approx \nu_B/\gamma\theta^2$, the same estimate gives $F_\nu \sim \nu^{\sigma}\theta^{2\sigma}/B^{\sigma-1}$ using the other limiting radiation pattern $\Delta\psi \approx \theta$. Note that the highest energy electrons dominate also the lowest energy emission. The two limiting slopes meet at the cyclotron turnover ν_B/θ, a fair estimate of the position of the power maximum. For uncorrelated γ and θ, a microscopic average over the effective pitch angle distribution is to be taken, cf. also O'Dell and Sartori 1970.

c) The range of the emitted spectrum is not necessarily given by the full range in electron energy. On the one hand, correlations between energy and angle tend to be built up by energy gain and loss processes in the sense of higher γ going together with smaller θ. If $\gamma\theta^2 \approx$ const, piling up of radiation at the l.f. edge will steepen the spectrum; if $\gamma^2\theta \approx$ const, the same effect

occurs at the h.f. limit. On the other hand, the assumption of uniform B may well be too schematic; both acceleration and energy loss can depend on position, thus modifying the spectrum; the different dependences on B of the l.f. spectrum ($\sim B^{-\sigma+1}$) and of the h.f. spectrum ($\sim B^{\frac{\sigma+1}{2}}$) weight differently contribution from low and high B regions. Also, dependence of self-absorption on spreads in γ and θ should be considered; moreover, beam visibility conditions in a well ordered geometry tend to reduce the contribution of high energy electrons.

A precise determination of spectral shapes will require further consideration. We conclude at this stage that the key departures from past schemes are: First, a l.f. cut-off can appear in optically thin conditions at reasonable values of the magnetic field; namely, the frequency ν_0/θ is larger than the synchrotron self-absorption if

$$\frac{B^2}{\theta^3} > 300 \frac{S_m}{\alpha^2} \qquad (2)$$

where S_m is the flux at the observed turnover, and α is the observed angular width of the source. Second, the h.f. cut-off is lowered at least to $\approx \nu_0 \gamma_2^2 \theta$. Third, there is a qualitative tendency to shrink the spectral range still further. The gross features of the IR peak can thus be explained by synchrotron emission from optically-thin electrons, moving at small pitch angles within a moderately high B, near large (even single) anchoring masses.

We now fix those magnitudes which do not strongly depend upon the IR spectral shape. First of all, the transit-time arguments set the diameter of the emitting region at 10^{16} cm, a smaller size than that derived from the current angular resolution of VLBI. We place the emitting volume at 10^{47} cm^3.

The total synchrotron power is given by:

$$P \approx 10^{47} \text{ or } 10^{48} \text{ erg} \approx 3\ 10^{-15}\ B^2\ (\gamma\theta)^2\ nV$$

where n is the mean number density of relativistic electrons. The frequency of peak power , not well known, is given by the cyclotron turnover frequency $\frac{\nu_B}{\theta} \approx 10^{12}$ or 10^{13} Hz. One additional relation is provided by the requirement that the magnetic fields preserve the form of the region, so that the magnetic stress must dominate the electron loss stress, giving $B^2/4\pi m n c^2 \gamma > 1$. Moreover, for the correct use of the synchrotron relations, we must require that $(\gamma\theta) > 1$ for all γ. A consistent set of parameters is given by $B \approx 10^4$ Gauss and $n = 10^7$ or 10^8 cm^{-3}. To exhibit separately the values of γ and the pitch angle, we choose a pair, not for the cyclotron peak power frequency, but for say 10^{14} Hz, with the usual relation $\nu_{cr} = \frac{1}{2} \nu_B \gamma^2 \theta \approx 10^{14}$ Hz Such electrons then have an energy $\gamma \approx 10^3$ and a pitch angle $\theta \approx 10^{-2}$. The low-energy electron cut-off γ_1 will reasonably be some tens; the overall range of the electron spectrum is then about $\gamma_2/\gamma_1 \approx 30$ to 50 . The mass flow works out to some 10 $M_\odot$/year (taking one proton per electron). In section 5 we will show that this size, stress ratio, mass flow, and magnetic field all fit naturally into the framework of our dynamical model.

Angular concentration of the source, and the likelihood of short term, strong fluctuations are known, interesting properties of a collimated (on the average) geometry of the emitting particles (Woltjer 1966).

4. The next high frequency bands of the spectrum, the optical

and possibly the X-ray continua, can arise from inverse Compton scattering of the same IR photons by energetic electrons. The ratio of inverse Compton to parent synchrotron power (Woltjer 1966) can be expressed as

$$\frac{P_c}{P_s} \approx \gamma'^2 \sigma_T n' L' \theta'^4$$

where L is the length of the regions, θ' is the angle between electrons and photons, the index ' applies to the region where the scattering actually takes place, which is not necessarily coincident with the region of synchrotron photon generation; $\sigma_T = \frac{8\pi}{3}\left(\frac{e^2}{mc^2}\right)^2$ is a fair estimate of the cross section as long as $\gamma' h\nu \ll mc^2$. Notice that the opacity to Compton scattering $\sigma_T n' L' \theta'^4$ is appreciable for large* objects where $nL \approx 10^{23}$ to 10^{24} cm^{-2}, unless the angle θ' stays very small. The gain in energy of single photons is of order γ'^2, unless again the angle is very small. Successive scatterings will extend the spectrum weakly up to $\gamma' h\nu \approx mc^2$, where the cross section declines.

Thus an average curvature of the lines of B will inevitably start a Compton cascade, if not at the IR emission region itself, then slightly beyond it, where synchrotron photons from other regions of the source encounter the electrons moving nearly along B under a substantial collision angle. The synchrotron life time being short compared with the transit time, the

*In contrast to sources with much larger surface-to-volume ratio like the circumpulsar region in Crab Nebula.

energy, spectral distribution, and total output of the Compton photons will depend sharply upon the relative position (or overlapping) of the acceleration and the emission regions.

We take a few steps more on the assumption that $\gamma' \lesssim \gamma$ and $\theta' \gg \theta$. Then the inverse Compton photons extend over a range fixed by that of the primary electrons, $(\gamma_2/\gamma_1)^2$. In the γ, θ correlated model for the IR emission one finds $\gamma_2/\gamma_1 \approx 30 - 50$, and hence would expect inverse Compton photons extending over three decades, starting with about 10^{15} Hz. One expects an X-ray continuum with a shape like the optical one, about $1/\nu$. Notice also that the cross-section decline would begin at $\nu \approx 10^{21}/\gamma'$ Hz; the spectrum ought not to persist into the gamma ray region, neither on the basis of the IR bandwidth nor from total energy arguments. The unseen bands between the visible and the keV X-rays must also contribute output power, for the most part absorbed in the gas of any surrounding galaxy, which is a few times the observed optical power.

At the other extreme of the range of electron parameters, we expect an excess of low-energy electrons with $\gamma\theta \lesssim 1$; which contribute a narrow IR peak roughly at ν_B/θ, while the high energy electrons generate an optical synchrotron continuum, and the Compton photons become unimportant. Such a spectrum would not flatten markedly going from IR to the optical band, would extend much less far into the X-ray region, and might tend to a higher polarization in the visible than in the IR.

5. The above emission scheme, although in principle independent, fits very well with qualitative and quantitative features of the spinar dynamical model (Morrison 1969; Cavaliere, Pacini, Setti 1969; Cavaliere 1970; Woltjer 1970) for the cores of violent sources.

The main links are the strength of the magnetic field, its extent and curvature, the continuous acceleration of electrons, the overall energetics and the mass loss.

The model independently requires fields about 10^5 G at the surface of the spinar, some 10^{15} cm in radius; the general poloidal field varies outwards with a law between the extremes $\frac{1}{r^2}$ and $\frac{1}{r^3}$ (or steeper for multipoles higher than dipole), as the stress ratio increases. In this framework, the IR region would be located within the critical surface, with radius $r \approx \frac{c}{\Omega} \ll 10^{17}$ cm, say close to 10^{16} cm. In rotating models, the poloidal $\underline{B}$ develops gradually into a toroidal component at the critical surface, so that electrons are certain, at least there, to collide with photons at non-negligible angle. Continuous and efficient acceleration of electrons, electrostatic and electromagnetic, is predicated by the model, if only by analogy with the pulsar; though the details of the acceleration are not understood, large-scale, strong electric fields are expected at least within the critical surface. The dynamical and e.m. stresses corresponding to the mass loss cause the body to lose angular momentum and hence to evolve by continuously releasing gravitational energy; first, into rotational energy; and therefrom efficiently into particle and e.m. energy, by way of the $\underline{B}$ field. The thermal energy content always remains small.

Note that a continuous release of 10^{48} erg/s of rotational energy, by flow of mass and of e.m. angular momentum; $10^{48} \approx c \frac{B_c^2}{4\pi} 4\pi \left(\frac{c}{\Omega}\right)^2$, implies a field B_c at the critical surface of about 10^3 Gauss, again corresponding to 10^4 or 10^5 Gauss at the surface. The energetic content of the magnetosphere amounts to about 10^{55}

erg; such plasma energies are associated with the larger radio bursts. On the other hand, the core is bound to emit mass discontinuously, with an average period something like the rotational period $T \approx 1$ year, whenever dynamically excited. The weak-field radio burst phenomena correspond to the expansion of these lumped mass ejections, in the way proposed by van der Laan (1966). The radio bursts, therefore, while sharing a common energetic origin with the other spectral bands, are not strictly time-correlated with them, since the radio emission arises only far beyond the critical surface, when the magnetic field is well under 1 Gauss. Radio-silent QSO'S have a cyclotron turnover cut-off but currently no radio clouds. Rees (1970) has already pointed out the possible continuity of the radio burst clouds with the filaments causing the multiple absorption red shifts familiar in large-z quasars (see also Shklovskii 1969). Optical jets and wisps, and extended multiple radio structures imply instead occasional, major disruptions of a spinar into secondary objects, themselves often sources.

Outside the critical surface, $B \sim r^{-1}$; if adiabatic invariance at constant energy prevails, $B_\perp \sim r^{-3/2}$. We anticipate that electrons leaking from the critical surface emit a steady synchrotron background of about 10^{46} ergs in the millimeter range, falling in intensity with increasing frequency.

It is not hard to see that the idea of a coherent spinning object whose magnetic field decreases with distance according to a power law implies a power law energy distribution for fast protons, once we suppose that the sites of injection are

more or less uniformly spread along the radius. A similar model for electrons, of course, must take into account the radiative losses. One may estimate very crudely the maximum energy for electrons by considering the external field beyond the light circle as a wholly non-accelerating magnetic region (Landau and Lifschitz 1962). That estimate yields a maximum electron energy 10^2 GeV; this implies that the emitted e.m. spectrum will not continue beyond $h\nu \lesssim 20$ MeV without a break.

We are very grateful to our MIT colleagues, Mr. S. O'Dell and Prof. Sartori, for telling us of the cyclotron turnover phenomenon before publication, to Dr. T. Kinman and Prof. N. Visvanathan for encouraging information on their unpublished optical studies of 3C345, and to Prof. B. F. Burke and L. Woltjer for much discussion and helpful comments.

REFERENCES

Aumann, H. H., and Low, F. J. 1970, Ap. J. (Letters), 159, L159

Becklin, E. E. and Ne-gebauer, G. 1969, Ap. J. (Letters), 157, L31.

Bowyer, C. S., Lampton, M., Mack, J. and DeMendonca, F. 1970, preprint.

Burbidge, G. R. and Burbidge, E. M. 1967, Quasi-Stellar Objects (San Francisco: W. H. Freeman & Co.).

Cavaliere, A. 1970, to be published in Proceedings of Symposium on Pulsars and High Energy Activity in Supernova Remnants, Rome, December 1969.

Cavaliere, A., Pacini, F., and Setti, G. 1969, Ap. Letters, 4, 103.

Friedman, H., to be published.

Hoerner, S. von 1966, Ap. J. 144, 483.

Johnson, H. L., and Low, F. J. 1965, Ap. J. 141, 336.

Kellermann, K. I., and Pauliny-Toth, I. I. K. 1968, Ann. Rev. Astr. and Ap., 6, 417.

Kellermann, K. I. and Pauliny-Toth, I. I. K. 1969, Ap. J. (Letters) 155, L71.

Kellermann, K. I., Clark, B. G., Bare, C. C., Rydbeck, O., Ellder, J., Hanson, B., Kollberg, E., Hoglund, B., Cohen, M. H., and Jauncey, D. L. 1968, Ap. J. (Letters) 153, 1209.

Kleinmann, D. E., and Low, F. J. 1970, Ap. J. (Letters) 159, L165.

Laan, H. van der 1966, Nature, 211, 1131.

Landau, L. D., and Lifshitz, E. M. 1962, The Classical Theory of Fields, Revised Second Edition, p. 240 (Reading, Mass: Addison-Wesley Publishing Company, Inc.).

Low, F. J., and Kleinmann, D. E. 1968, A.J. 73, 868.

Morrison, P. 1969, Ap. J. (Letters), 157, L73.

O'Dell, S., and Sartori, L. 1970, preprint.

Oke, J. B. 1966, Ap. J. 145, 668.

Oke, J. B. 1968, A.J. 73, 849.

Osterbrock, D. E., and Parker, R. A. R. 1966, Ap. J., 143, 268.

Pacholczyk, A. G., and Weymann, R. J. 1968, A. J., 73, 870.

Pauliny-Toth, I. I. K., and Kellermann, K. I., 1968, Ap. J. (Letters), 152, L169.

Rees, M. J. 1970, Ap. J. (Letters), 160, L29.

Shklovskii, I. S. 1969, Astr. Zh. 46, 935 (English translation 1970, Sov. A. J., 13, 734).

Visvanathan, N. and Oke, J. B., Ap. J. (Letters) 152, L165, 1968.

Woltjer, L. 1966, Ap. J. 146, 597.

Woltjer, L. 1970, Semaine d'Etude, Les Noyaux des Galaxies, Pontifical Academy of Sciences, Rome, to be published.

Caption to Figure

Fig. 1 - Schematic diagram of a typical strong source (not to scale). The numbered regions are described below:

0 Spin axis: spinar with angular momentum J, mass 10^9 $M_\odot$; $\Omega \sim 10^{-7}$ or 10^{-8} s^{-1}.

1 Surface of spinar: poloidal field enhancement.

2 Synchrotron emission of IR.

3 Compton-recoil emission of optical and x-ray continua.

4 Critical surface-- $r \approx c/\Omega$.

5 Radio burst clouds, r.f. emission, $\lambda < 1$ m (expanding as they move out) (van der Laan 1966).

6 Emission-line optical source, excited gas filaments (Osterbrock and Parker, 1966).

7 Absorption-line optical source, fast-moving cooled gas filaments (Rees 1970).

8 Weak-field synchrotron plasma, r.f. mainly $\lambda > 1$m.

Particle acceleration continues throughout region 2, and perhaps beyond.

The general B field falls about as $1/r^2$ or $1/r^3$ until the critical surface; outside that, it is mainly toroidal, and falls as $1/r$. The whole volume is traversed by the large output of relativistic protons.

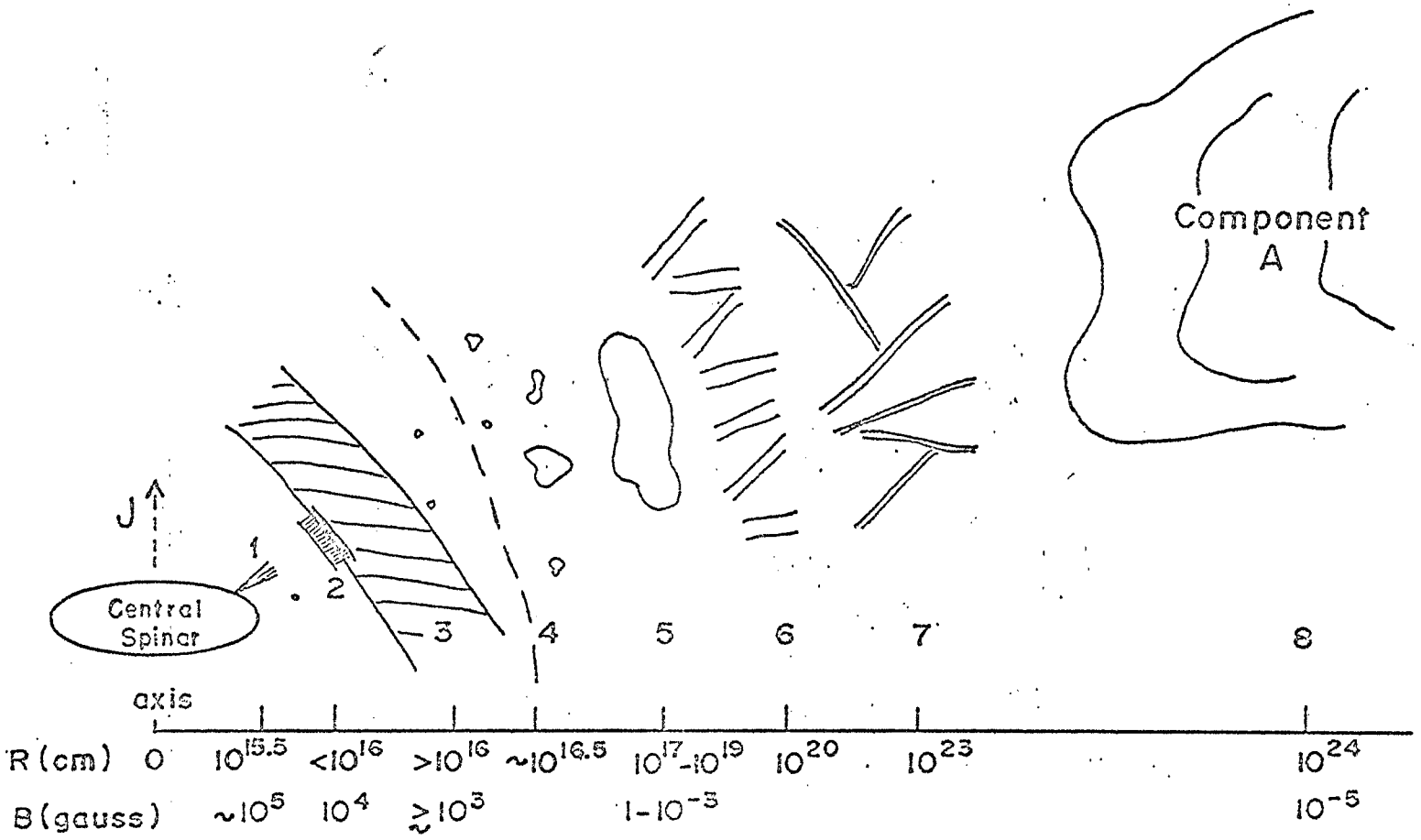
Component
A
J
1
2
3
4
5
6
7
8
Central
Spinar
axis
R (cm) 0 $10^{15.5}$ $<10^{16}$ $>10^{16}$ $\sim10^{16.5}$ 10^{17}-10^{19} 10^{20} 10^{23} 10^{24}
B (gauss) $\sim10^{5}$ 10^{4} $\gtrsim10^{3}$ 1-10^{-3} 10^{-5}